Carcinogenesis vol.33 no.9 pp.1639–1646, 2012
doi:10.1093/carcin/bgs195
Advance Access Publication June 7, 2012

Epithelial–mesenchymal transition increases tumor sensitivity to COX-2 inhibition by apricoxib

Amanda Kirane[1,2], Jason E.Toombs[1,2], Jill E.Larsen[2], Katherine T.Ostapoff[1,2], Kathryn R.Meshaw[3], Sara Zaknoen[4], Rolf A.Brekken[1,2] and Francis J.Burrows[4,*]

[1]Department of Surgery, Division of Surgical Oncology and [2]Hamon Center for Therapeutic Oncology Research, University of Texas Southwestern Medical Center, Dallas, TX , 75390 USA, [3]Charles River Laboratories, Morrisville, NC, 27560 USA and [4]Tragara Pharmaceuticals, Inc, San Diego, CA 92130, USA

*To whom correspondence should be addressed. Tragara Pharmaceuticals, 10955 Vista Sorrento Parkway, Suite 120, San Diego, CA 92130, USA.
Tel: 858 350 6935; Fax: 858 350 6920;
Email: fburrows@tragarapharma.com

Correspondence may also be addressed to Rolf A. Brekken, Hamon Center, UT Southwestern Medical Center, 6000 Harry Hines Blvd, MC8593, Dallas, TX, 75390 USA. Tel: 214 648 5151; Fax: 753 908 593;
Email: rolf.brekken@utsouthwestern.edu

Although cyclooxygenase-2 (COX-2) inhibitors, such as the late stage development drug apricoxib, exhibit antitumor activity, their mechanisms of action have not been fully defined. In this study, we characterized the mechanisms of action of apricoxib in HT29 colorectal carcinoma. Apricoxib was weakly cytotoxic toward naive HT29 cells *in vitro* but inhibited tumor growth markedly *in vivo*. Pharmacokinetic analyses revealed that *in vivo* drug levels peaked at 2–4 µM and remained sufficient to completely inhibit prostaglandin E_2 production, but failed to reach concentrations cytotoxic for HT29 cells in monolayer culture. Despite this, apricoxib significantly inhibited tumor cell proliferation and induced apoptosis without affecting blood vessel density, although it did promote vascular normalization. Strikingly, apricoxib treatment induced a dose-dependent reversal of epithelial–mesenchymal transition (EMT), as shown by robust upregulation of E-cadherin and the virtual disappearance of vimentin and ZEB1 protein expression. *In vitro*, either anchorage-independent growth conditions or forced EMT sensitized HT29 and non-small cell lung cancer cells to apricoxib by 50-fold, suggesting that the occurrence of EMT may actually increase the dependence of colon and lung carcinoma cells on COX-2. Taken together, these data suggest that acquisition of mesenchymal characteristics sensitizes carcinoma cells to apricoxib resulting in significant single-agent antitumor activity.

Introduction

Inflammation has recently been described as an enabling characteristic that can drive many of the 'hallmarks of cancer' (1). Cyclooxygenase-2 (COX-2) is an immediate early response gene that is typically not expressed in resting cells but is highly inducible by growth factors and inflammatory cytokines (3). COX-2 is the rate-limiting enzyme in the production of prostaglandins, primarily prostaglandin E_2 (PGE_2), from arachidonic acid (3) in epithelial tumor cells and stromal cells such as endothelial cells and macrophages (4,5). COX-2 is overexpressed in many solid tumors, most prominently colorectal carcinoma (CRC), non-small cell lung cancer (NSCLC), pancreatic and head and neck cancer (6). PGE_2 promotes tumor growth and survival by regulating tumor cells and their complex interaction with the nurturing stroma (3). Elevated PGE_2 increases tumor proliferation in CRC and NSCLC via the extracellular signal-regulated kinase, src and β-catenin pathways (7–9) and enhances survival signaling via the Akt and nuclear factor-kappaB pathways, which upregulate antiapoptotic proteins of the Bcl-2 family (2,10). PGE_2 also stimulates neovascularization, invasion and metastasis and blunts cell-mediated antitumor immunity (6).

Celecoxib and other COX-2 inhibitors have been studied extensively in preclinical models of cancer. Although this class of drugs show potent antitumor activity *in vivo* (11,12), several groups have reported that the concentrations—20–100 µM—required to mediate direct antiproliferative or proapoptotic effects toward human cancer cells *in vitro* (12–14) are substantially in excess of the blood or tissue levels achievable in animals or humans (1–4 µM for celecoxib) (11,15). These results suggest that the *in vivo* antitumor activity is realized primarily or exclusively via indirect, host-dependent processes, such as inhibition of angiogenesis (11). Celecoxib may also have important off-target activity, such as blocking Akt signaling (16), which may be responsible for its direct *in vitro* effects on tumor cells.

Apricoxib is a novel COX-2 inhibitor currently in Phase II clinical trials in cancer (17). Apricoxib displays antitumor and antiangiogenic activity in human patients and several murine models of cancer (18,19), but its mechanisms of action have not been fully defined. The clinical development strategy for apricoxib employs a biomarker of activation of the COX-2 pathway, the urinary PGE_2 metabolite PGEM (20), as a method to select for patients with an active COX-2 pathway in their tumors. Therefore, it is important to determine whether the antitumor activity of apricoxib is mediated via the inhibition of COX-2-dependent PGE_2 production. Furthermore, the growing evidence implicating PGE_2 in the regulation of epithelial–mesenchymal transition (EMT) suggests that COX-2 inhibitors may affect this process, which is involved in metastasis (21).

In this study, we first characterized the activity of apricoxib in comparison to celecoxib, against a panel of human tumor xenografts *in vitro* and *in vivo* before focusing on the HT29 CRC model for a detailed analysis of the mechanisms underlying the antitumor activity of the drug. We present evidence that the true activity of apricoxib *in vitro* is discernable only when the target cells are manipulated to simulate *in vivo* progression to a mesenchymal phenotype. The primary mechanism of action, in the CRC and NSCLC models reported in this study, appears to be reversal of EMT associated with inhibition of tumor cell proliferation and survival.

Abbreviations: COX-2, cyclooxygenase-2; CRC, colorectal carcinoma; EMT; epithelial–mesenchymal transition; NSCLC, non-small cell lung cancer; PGE2, prostaglandin E2; TGF-β, transforming growth factor-β; VEGF, vascular endothelial growth factor.

Materials and methods

Cell culture

The human tumor cell lines were obtained from ATCC. Cell lines were confirmed to be pathogen free prior to use. Cells were grown in DMEM, RPMI-1640 or McCoy's modified medium (Sigma–Aldrich) and maintained at 37°C in a humidified incubator with 5–10% CO_2 and 90–95% air. For *in vitro* EMT experiments, cells were plated on collagen-coated tissue culture dishes and treated with 20 ng/ml transforming growth factor-β (TGF-β) (Peprotech) prior to 48 h incubation with apricoxib and fresh TGF-β in 2% serum media. Control cells were plated on plastic tissue culture dishes and treated for 48 h with apricoxib only.

In vitro *cytotoxicity and drug response assays*

MTS assays were performed in 96-well plates; cells were plated on day 0 and apricoxib was added on day 1 in fourfold dilutions with a maximum concentration of 500 µM. Relative cell number was determined 96 h later by adding MTS (Promega, final concentration 333 µg/ml), incubating for 1–3 h at 37°C and absorbance was read. Drug sensitivity curves and IC_{50} values were calculated using in-house software. Anchorage-independent growth assay was performed by coating 12-well plates with 0.5–0.75% agar. Cells were resuspended in 0.375% agar with apricoxib added in both soft agar layer and in media. Fresh media/drug was added twice weekly and colonies were measured

© The Author 2012. Published by Oxford University Press. All rights reserved. For Permissions, please email: journals.permissions@oup.com

Downloaded from https://academic.oup.com/carcin/article/33/9/1639/2463654 by guest on 25 April 2024

by light microscopy at 2 weeks; assays were performed in quadruplicate. *In vitro* PGE_2 and vascular endothelial growth factor (VEGF) response to apricoxib treatment was evaluated by enzyme-linked immunosorbent assay (ELISA; R&D Systems) of conditioned media over a 24-h incubation period.

Western blot and immunocytochemistry

Cell lines were plated in 100 mm^3 dishes and grown to 90% confluency. Cells were harvested for lysate using MPER (Pierce) with added protease and phosphatase inhibitors. Protein concentration was determined by BCA assay (Pierce). Protein immunodetection was performed by electrophoretic transfer of sodium dodecyl sulfate–polyacrylamide gel electrophoresis separated proteins to polyvinylidene difluoride membrane. Antibodies used to probe membranes included ZEB-1, E-cadherin, proliferating cell nuclear antigen (PCNA; Santa Cruz), phospho-histone H3 (Upstate), cleaved caspase-3 and cleaved poly (ADP ribose) polymerase (PARP; Cell Signaling). Immunocytochemistry was performed by incubating cells overnight in cell culture chamber slides and fixing in 4% formalin. About 0.5% Brij was used to permeabilize cells, which were then evaluated for cleaved caspase-3, ZEB-1 and E-cadherin. Negative controls were performed by omitting the primary antibody. Slides were incubated with fluorophore-conjugated secondary antibody (Jackson Immunoresearch) and Prolong with Dapi (Invitrogen). Sections were examined on a Nikon E600 microscope, and images were captured with Photometrics Coolsnap HQ camera using Elements Software. Conditions for exposure time remained constant and images were thresholded to exclude background signal.

Histology and immunohistochemistry

Formalin-fixed tissues were embedded in paraffin and cut in 10-micron sections. Tissue sections were deparaffinized and rehydrated in phosphate-buffered saline containing 0.2% Tween-20 prior to staining. Sections were blocked in 20% AquaBlock (East Coast Biologics), incubated with primary antibody overnight at 4°C followed by fluorophore-conjugated secondary antibody (1:500) (Jackson Immunoresearch) for 1 h at room temperature and mounted with ProLong Gold antifade reagent with DAPI (Invitrogen). Antibodies used include CD31 (Dianova), NG2 (Millipore), vimentin (Phosphosolutions), ZEB-1, E-cadherin, PCNA (Santa Cruz), phospho-histone H3 (Upstate), TUNEL (Promega), cleaved caspase-3 (Cell Signaling), VEGF and COX-2 (Abcam). Antigen retrieval was performed by boiling in citrate buffer in a pressure cooker for 20 min. Negative controls and immunofluorescent evaluation were performed as described for immunocytochemistry. Representative images were captured under identical conditions of magnification and exposure time. Images were thresholded to exclude background signal of secondary antibody alone. An average of 8 images/tumor was evaluated for each target (45).

HT29 xenograft model

All animals were housed in a pathogen-free facility with 24 h access to food and water. Experiments were approved by, and performed in accordance with, the IACUC at Charles River Laboratories (Morrisville, NC). In this study, 6–7-week-old female athymic nude mice (*nu/nu*, Harlan) were implanted subcutaneously with 1 mm^3 tumor fragments and tumors were allowed to establish to an average size of 93 mm^3 before initiation of therapy. Animals were treated orally daily with 10 or 30 mg/kg apricoxib in 1% carboxymethyl cellulose (CMC) in DI water, tumor growth was measured biweekly by caliper measurement and volume was calculated using the formula: Tumor volume = $w2 \times l$, where w = width and l = length in millimeter of the tumor.

Cetuximab (Erbitux®, Bristol-Myers Squibb, Lot No. 071003108) was dosed at 20 mg/kg biweekly intraperitoneally in 0.9% NaCl. Methods for the other xenograft models are described in the Supplementary section.

Apricoxib pharmacokinetics

For determination of apricoxib pharmacokinetics in mouse plasma and subcutaneous tumors, HT29 tumors were seeded as above and allowed to grow to 300–500 mm^3 before tumor-bearing animals received a single oral dose of 10 or 30 mg/kg apricoxib. Blood was collected into K_2-ethylenediaminetetraacetic acid tubes by cardiac puncture under CO_2 anesthesia at 0.5, 1, 2, 3, 6, 16 and 24 h after dosing and stored at −80°C for subsequent determination of plasma concentrations of apricoxib or murine VEGF. Tumors were excised at the same timepoints and snap-frozen over liquid nitrogen for subsequent determination of intralesional concentrations of apricoxib. Plasma and tumor drug concentrations were determined as follows: mouse tumor samples were pulverized with Covaris CryoPrep (CP-02), diluted 1:5 in water and homogenized/mixed with Covaris for 4 min. About 50 µl volumes of control matrix, QC samples (mouse plasma assay only) or study samples (mouse plasma or mouse tumor homogenate) were placed in individual 1.5-ml Eppendorf tubes along with 50 µl of 50% methanol, calibrators, 50 µl of internal standard working solution (R-133185 at 200 ng/ml) and 200 µl of methanol was added to each tube and vortexed gently. The samples were then centrifuged at 13 000 rpm for 10 min at room temperature. A portion of resulting supernatant (250 µl) was transferred into an injection vial with insert and 10 µl sample was injected onto an API 4000 liquid chromatography/mass spectrometry system. Mass spectral analysis was conducted using a Sciex API 4000 mass spectrometer coupled to a Shinadzu high-performance liquid chromatography system. The mass spectrometer was operated in the positive ionization mode using an electrospray ionization interface. Data acquisition was conducted using Analyst software (version 1.4.2).

For pharmacodynamic analyses, HT29 tumors were seeded as for the therapy experiment, allowed to establish to a size of ~150 mm^3, and tumor-bearing animals were treated orally daily with 10 or 30 mg/kg apricoxib in 1% CMC in DI water for 3 weeks. Tumors were either fixed in 10% formalin or snap-frozen in liquid nitrogen for further studies. Human and mouse VEGF levels of serum and tumor were determined by ELISA kit (R&D Systems).

Statistics

Data were analyzed using GraphPad software (GraphPad Prism version 3.03 or 4.00 for Windows; GraphPad Software, San Diego, CA, www.graphpad.com). Results are expressed as mean ± standard error of the mean (SEM). Data were analyzed by *t*-test or analysis of variance (ANOVA) and results are considered significant at $P < 0.05$.

Results

Apricoxib possesses antitumor activity in vitro and in vivo

In preliminary experiments, the antitumor activity of apricoxib was determined in a panel of human tumor models *in vitro* and *in vivo*. To determine the potency of apricoxib and celecoxib *in vitro*, tumor cells were seeded in log-phase growth in 96-well plates and exposed to a titration of the COX-2 inhibitors for 4 days before the residual cell number was estimated by methylene blue assay, which detects inhibition of proliferation and cytotoxic activity. Under these standard conditions, COX-2 inhibitors exhibited modest but highly consistent activity; the mean IC_{50} for apricoxib was 37.2 ± 6.2 µM (range 23–100 µM) and 27.9 ± 2.7 µM (range 22–57 µM) for celecoxib, suggesting that these effects were mediated by a conserved mechanism that manifests similarly in a range of different cell types (Supplementary Table 1, available at *Carcinogenesis* Online).

Next, we tested apricoxib under a standard regimen (30 mg/kg daily oral gavage) in a series of xenograft models. Apricoxib as a single agent demonstrated significant antitumor activity in 3/3 NSCLC xenografts, 1/2 CRC models and in melanoma and glioblastoma tumors but was inactive in 3/3 breast cancers, although it was significantly active in combination with standard of care drugs such as trastuzumab in a HER2+ breast cancer model and pemetrexed in a triple-negative xenograft (Supplementary Table 2, available at *Carcinogenesis* Online). The most robust single agent activity was seen in the cetuximab-resistant, BRaf-mutant CRC HT29, so this model, which has been studied extensively in relation to COX-2 (12,22), was selected to characterize the mechanisms of antitumor activity of apricoxib.

Apricoxib is enriched in tumor tissue and inhibits COX-2 activity and tumor growth in the HT29 model

To determine the biodistribution of apricoxib, HT29 tumor-bearing mice were given a single oral gavage of apricoxib (10–30 mg/kg). Apricoxib was rapidly absorbed at both dose levels—maximum concentrations in blood and tumor were achieved in 30–60 min (Figure 1A). Peak levels in animals receiving 10 mg/kg were 5522 nM in plasma and 2051 nM in tumor tissue versus 10 526 nM in plasma (data not shown) and 4356 nM in tumor tissue in animals receiving 30 mg/kg. Blood apricoxib levels declined rapidly to below 200 nM in 8–12 h and <10 nM by 24 h, but remained elevated in tumor tissues for the duration of the 24-h dosing period; trough levels were 142 and 382 nM at 10 and 30 mg/kg, respectively.

Inhibition of COX-2 activity was measured *in vitro* using an ELISA for the COX-2 pathway product PGE_2. Apricoxib rapidly and irreversibly inhibited PGE_2 secretion by HT29 cells, with levels in the culture medium dropping 90% below baseline within 6 h and reaching negligible levels by 24 h (Figure 1B). PGE_2 is highly unstable *in vivo*, so

Downloaded from https://academic.oup.com/carcin/article/33/9/1639/2463654 by guest on 25 April 2024

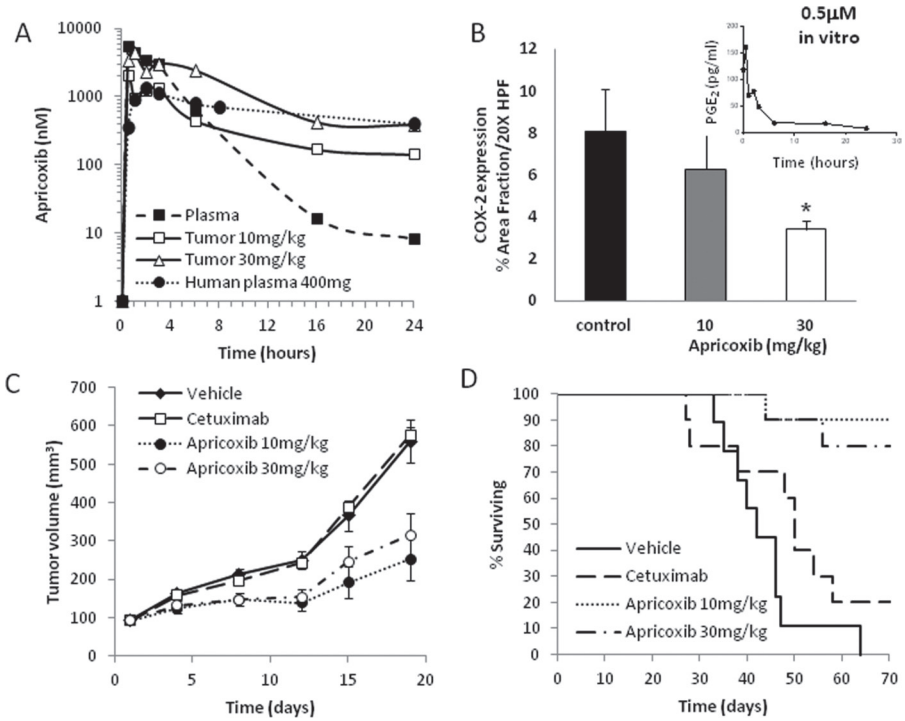

Fig. 1. Pharmacokinetics, target inhibition and antitumor activity of apricoxib. **(A)** Concentrations of apricoxib in the plasma (solid squares, dashed line) or tumor tissue (open symbols, solid lines) of HT29 tumor-bearing nude mice after a single oral dose of 10 (squares) or 30 (triangles) mg/kg were determined using high-performance liquid chromatography mass spectrometry analysis. Also shown for comparison is the concentration of apricoxib in the plasma of human patients after a single 400 mg oral dose of apricoxib (solid circles, dotted line). Data are the mean of readings from three animals; errors were 6–32% of the mean and are not shown. **(B)** Pharmacodynamic response in tumor tissue. HT29 tumor-bearing mice were treated with vehicle or apricoxib (oral, daily 21×) and tumors were stained with an anti-COX-2 antibody. Data are displayed as mean ± SEM and represents 5 images per tumor with 5 tumors per group evaluated. $*P \leq 0.02$ versus control by one-way ANOVA. Inset: Time course of inhibition of PGE_2 production by HT29 cells *in vitro* after exposure to apricoxib (0.5 μM). HT29 tumor-bearing nude mice were randomized into 4 groups of 10 animals each. Mice were treated for up to 70 days with vehicle (1% CMC), apricoxib (daily oral) or cetuximab (biweekly I.P.) as indicated. Effects on tumor growth rate **(C)** and animal survival **(D)** are shown.

levels of the prostaglandin could not be measured in plasma or tumor tissue (data not shown). Instead, COX-2 expression levels in tumor tissue were used as an indicator of pathway interdiction, as described previously (23,46–48). PGE_2 transactivates the gene for COX-2 (8), but there are many other pathways leading to COX-2 upregulation (3), so it was not entirely surprising that the effects of apricoxib were dose-dependent but relatively modest. Mean COX-2 expression levels in sections of excised tumors were reduced by 22% and 58% ($P < 0.02$) at doses of 10 and 30 mg/kg, respectively. Reduction in COX-2 expression was confirmed in tumor lysates by western blot (Supplementary Figure 1, available at *Carcinogenesis* Online).

Both 10 and 30 mg/kg doses of apricoxib suppressed tumor growth, by 65.6% ($P < 0.003$) and 52.5% ($P < 0.016$), respectively (Figure 1C). Apricoxib treatment also significantly extended survival; although all vehicle-treated animals succumbed between 33 and 64 days into the experiment, 9/10 and 8/10 animals treated with apricoxib at doses of 10 and 30 mg/kg, respectively, remained alive after 70 days ($P < 0.0006$) (Figure 1D). Cetuximab did not display any antitumor activity, probably due to the mutant BRaf expressed by HT29, which confers resistance to antiepidermal growth factor receptor monoclonal antibodies (24). Combinations of apricoxib and cetuximab were no more active than apricoxib alone (data not shown).

Apricoxib inhibits tumor cell proliferation, survival and anchorage-independent growth

The effects of apricoxib on growth of HT29 cells *in vitro* were compared under several conditions. Apricoxib was weakly active in cultures of HT29 cells grown under standard monolayer conditions in the MTS assay (IC_{50} ~ 43 μM, Supplementary Table 1, available at *Carcinogenesis* Online), but it was considerably more potent against the same cells grown under anchorage-independent conditions (IC_{50} ~ 0.5 μM) (Figure 2A). Because silencing of the EMT-associated transcription factor ZEB-1 also selectively suppressed anchorage-independent growth of epithelial tumor cells (25), we determined the sensitivity of HT29 cells to apricoxib that had undergone forced EMT26. Under these conditions, the cells lost expression of the epithelial adhesion protein E-cadherin and gained expression of the mesenchymal markers ZEB-1 (as shown in Figure 5A) and N-cadherin (data not shown). HT29 cells that had undergone EMT were compared with control cultures by western blot for PCNA expression, revealing that proliferation of EMT^+ HT29 cells was profoundly inhibited at concentrations as low as 500 nM apricoxib (Figure 2B). To determine whether *in vitro* growth conditions could alter sensitivity to apricoxib in other cancer cells, we titrated apricoxib against a panel of ZEB-1^{high} (EMT^+) and ZEB-1^{low} (EMT^-) NSCLC lines (25) grown under monolayer or anchorage-independent conditions. All seven NSCLC lines were resistant to apricoxib under standard culture conditions (mean IC_{50} 70.15 μM, range 38–95 μM) (Figure 2C). In contrast, 4/6 lines that formed colonies in soft agar responded to the drug, with two lines displaying values in the nanomolar range, confirming the observation in the HT29 model. Interestingly, all four of the lines that were highly sensitive to apricoxib were ZEB-1^{high} lines, suggesting that growth and survival of two kinds of EMT^+ carcinoma cells under anchorage-independent conditions is dependent upon COX-2.

In accordance with the potent antiproliferative activity seen in the clonogenic assays and forced EMT cultures, apricoxib dose-dependently inhibited HT29 tumor cell proliferation *in vivo*. Staining for the mitotic marker phospho-histone H3 was reduced by 32% and 89% ($P < 0.0001$) in tumors from animals treated with 10 and 30 mg/kg, respectively (Figure 2D and 2E). The proapoptotic

Downloaded from https://academic.oup.com/carcin/article/33/9/1639/2463654 by guest on 25 April 2024

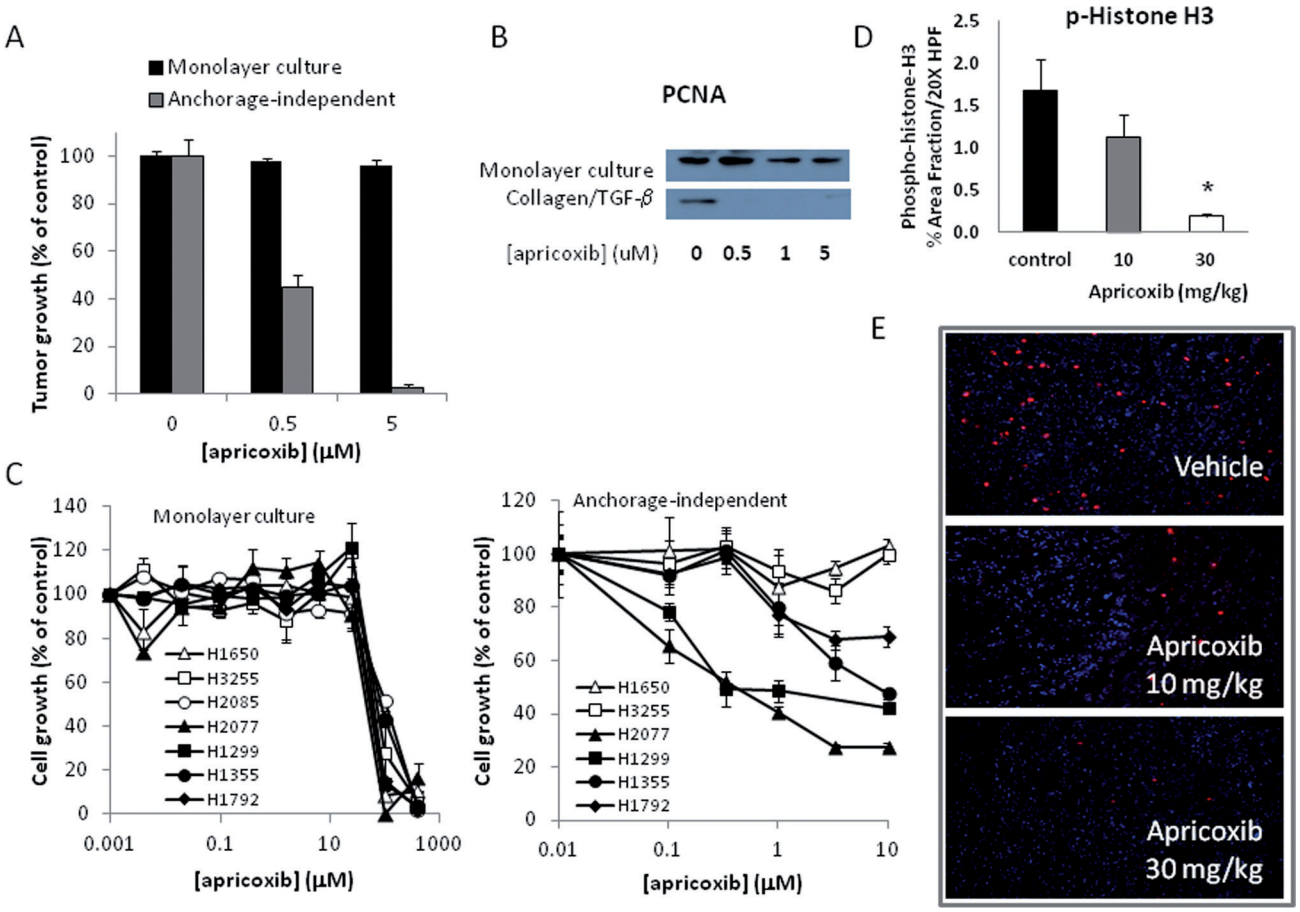

Fig. 2. Apricoxib inhibits tumor cell proliferation *in vitro* and *in vivo*. Inhibition of proliferation in monolayer culture (black bars in A, left panel in C) or under anchorage-independent conditions (gray bars in A, right panel in C) of HT29 cells **(A)** or NSCLC lines **(C)** was determined using the MTS assay or clonogenic assay, respectively. Cells were seeded in log-growth phase, treated with serial dilutions of apricoxib in quadruplicate and cell or colony number determined 4 (MTS) or 14 (clonogenic assay) days later. **(B)** Apricoxib-induced changes in PCNA expression were determined by western blot in cultures of HT29 cells grown under standard conditions (top panel) or following growth on a collagen matrix in the presence of 20 ng/ml TGF-β (bottom panel). **(D)** HT29 tumor-bearing mice were treated with vehicle or apricoxib (oral, daily 21×) and tumors were stained with an antiphospho-histone H3 antibody. Data are displayed as mean ± SEM, total magnification ×200 (B); *$P \leq 0.0001$ versus control by *t*-test. Representative images are also shown **(E)**.

activity of apricoxib *in vitro* was also altered by the EMT status of the cells. Under resting conditions, 20–40 μM concentrations of apricoxib were required to induce apoptosis in HT29 cells (data not shown), but apricoxib in the 0.5–5 μM range readily killed cells grown on collagen in the presence of TGF-β, as indicated by PARP cleavage and caspase-3 activation (Figure 3A and 3B). Similarly, apricoxib was strongly apoptotic in subcutaneous HT29 xenografts. As shown in Figure 3C, apricoxib significantly induced apoptosis in treated tumors at both dose levels ($P < 0.0005$ and $P < 0.0041$ at 10 and 30 mg/kg, respectively) as determined by TUNEL, and these results were confirmed by IHC for cleaved caspase-3 (Figure 3D and 3E)

Apricoxib modulates VEGF signaling and increases vessel maturity in vivo

COX-2 inhibitors, including apricoxib, have been shown to exert antiangiogenic activity *in vitro* and *in vivo*, most commonly via inhibition of VEGF production by tumor or host stromal cells (4,19), so we sought to determine whether effects on the tumor vasculature contributed to the observed antitumor activity of apricoxib in the HT29 model. *In vitro*, the drug rapidly decreased VEGF production by HT29 cells but, interestingly, the effect was neither complete nor stable; VEGF secretion decreased by >50% within 1 h of exposure to apricoxib, remained similarly depressed for at least 16 h but returned to baseline levels by 24 h. These results suggest that HT29 cells possess COX-2-independent pathways to VEGF production, as reported previously (27) and that these collateral pathways can completely compensate for COX-2 inhibition over time (Figure 4A). Apricoxib is known to potently inhibit VEGF production by LPS-activated endothelial cells and macrophages (19). Accordingly, we found that host (murine) VEGF transiently disappeared from the circulation of HT29 tumor-bearing mice within an hour of oral administration of apricoxib (Figure 4B). Analogously to the previous experiment, COX-2-independent mechanisms apparently compensated in the host stroma also, because mouse VEGF levels returned and exceeded baseline indeed within 6 h after dosing, despite the persistence of therapeutic levels of apricoxib in the blood at this timepoint (Figure 1A). Furthermore, human VEGF levels were unaltered in HT29 tumors after 21 days of apricoxib treatment (Figure 4C), suggesting that either the matrix-bound VEGF pool was untouched by the drug treatment or, more probably, that the tumor cells had fully compensated for COX-2 inhibition as demonstrated *in vitro* (Figure 4A). Given the transience of the effects of each dose of drug in this model system, it was not surprising that microvessel density was unchanged after prolonged apricoxib treatment (Figure 4D). In contrast, drug treatment did alter microvessel maturity, as indicated by double-staining for CD31 and the murine pericyte marker NG2 (Figure 4E). When quantified, pericyte coverage (the ratio of $CD31^+$, $NG2^+$ vessels/ $CD31^+$) was increased from ~77% to >98% ($P \leq 0.02$) at both doses of apricoxib (data not shown).

Downloaded from https://academic.oup.com/carcin/article/33/9/1639/2463654 by guest on 25 April 2024

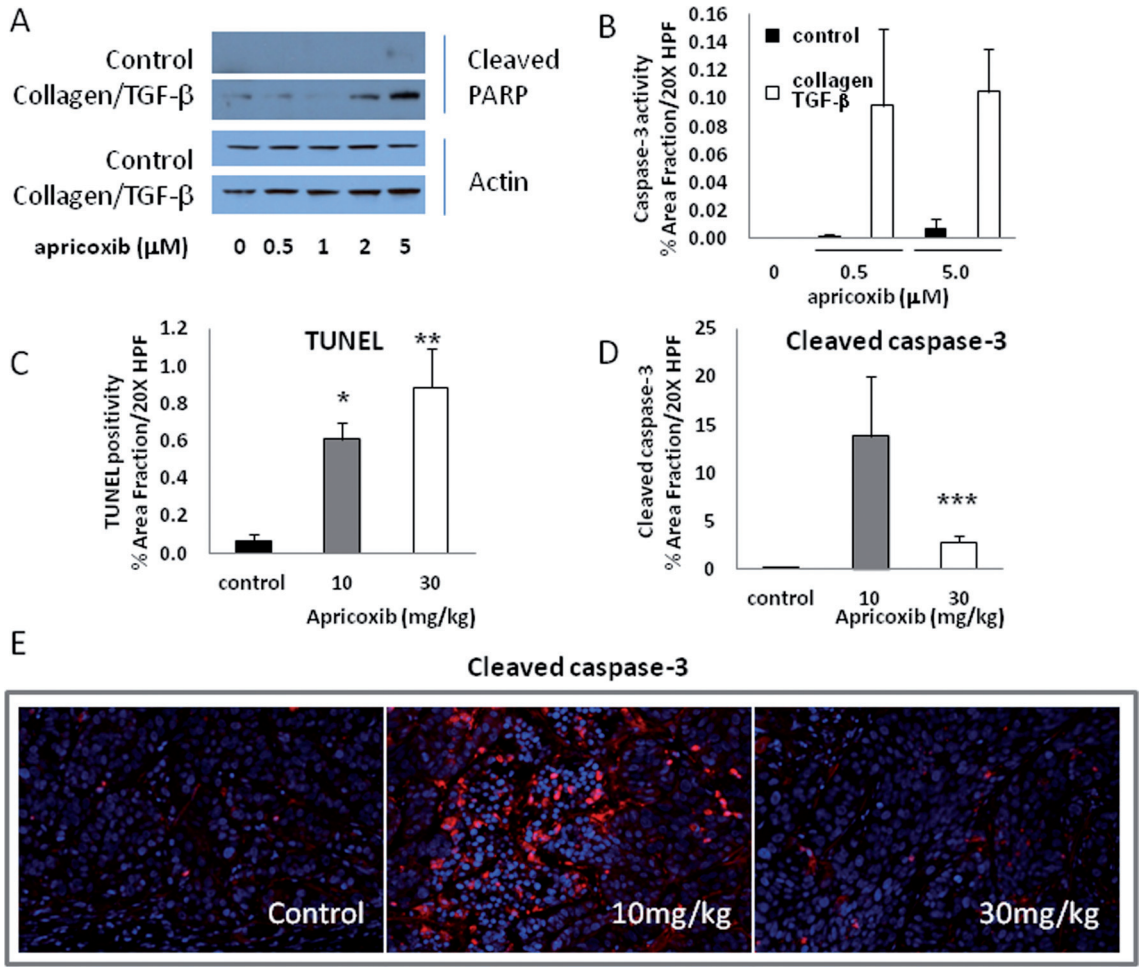

Fig. 3. Apricoxib induces tumor cell apoptosis *in vitro* and *in vivo*. Apricoxib-induced apoptosis *in vitro* was assessed by western blot for cleaved PARP **(A)** or immunocytochemistry with antibodies against cleaved caspase-3 **(B)** in cultures of HT29 cells grown under standard conditions or following growth on a collagen matrix in the presence of 20 ng/ml TGF-β. **(C–E)** HT29 tumor-bearing mice were treated with vehicle or apricoxib (oral, daily 21×) and tumors were stained by TUNEL **(C)** or with an antibody against cleaved caspase-3 **(D)**. Data are displayed as mean ± SEM, total magnification ×200 (B); $*P \leq 0.0005$, $**P \leq 0.0041$, $***P \leq 0.009$, versus control by *t*-test. Representative images are shown **(E)**.

Apricoxib reverses EMT in vitro *and* in vivo

HT29 cells display epithelial characteristics under standard culture conditions (28). However, prolonged growth on collagen-coated plastic in the presence of TGF-β induces the loss of the epithelial marker E-cadherin (Figure 5A) and the upregulation of the mesenchymal transcription factor ZEB-1 (Figure 5A and 5B). Under these conditions, EMT in HT29 cells is COX-2-dependent, as evidenced by the robust reversal of the process by apricoxib in the pharmacologically achievable 0.5–5 μM concentration range (Figure 5A and 5B). Importantly, growth of HT29 cells in the subcutaneous site in nude mice also precipitated EMT (29,30); established tumors expressed high levels of the mesenchymal intermediate filament protein vimentin but lacked E-cadherin (Figure 5F, top panel). As shown in Figure 5 (D–F), 21 days of treatment with apricoxib robustly and dose-dependently reversed EMT in this model; E-cadherin reappeared (Figure 5D and 5F) and vimentin (Figure 5E and 5F) and ZEB-1 (Figure 5F) were largely eradicated.

Discussion

Apricoxib is a potent, selective COX-2 inhibitor currently in Phase II clinical evaluation in NSCLC and pancreatic cancer (17). The clinical development strategy for apricoxib in oncology employs a novel biomarker of COX-2 activity to identify patients most probably to obtain clinical benefit, so this study was undertaken, to confirm that apricoxib exerts antitumor activity in human tumor model systems *in vitro* and *in vivo* via inhibition of the production of the oncogenic second messenger PGE_2; and to determine the critical downstream effects of inhibition of PGE_2 production that result in antitumor activity in solid tumor models.

In preliminary experiments, we confirmed that apricoxib possesses antitumor activity *in vitro* and *in vivo* but that, as described previously for celecoxib and other COX-2 inhibitors (11,14), direct antiproliferative and cytotoxic activity toward human cancer cells could only be achieved at concentrations of 20–50 μM *in vitro*. This inhibitory concentration is approximately 100-fold higher than needed to inhibit COX-2-dependent PGE_2 production in whole blood (31). To determine whether levels of apricoxib are sufficient to inhibit COX-2 and/or mediate direct antitumor effects were achievable in human tumor xenograft models, animals bearing the apricoxib-sensitive human CRC HT29 were treated with apricoxib and drug and COX-2 levels were measured throughout the 24-h dosing period in plasma and tumor tissue. Tumor levels of apricoxib peaked in the 2–4 μM range and declined to submicromolar concentrations during the course of the dosing interval. Direct measurement of PGE_2 levels in plasma and tumor lysate could not be achieved in this model due to rapid metabolism of PGE_2 *in vivo*. However, the positive feedback system by which PGE_2 regulates COX-2 production has been well established and validated at messenger RNA and protein levels (23,46–48). Thus, COX-2 expression is diminished following administration of COX-2 inhibitors and COX-2

Downloaded from https://academic.oup.com/carcin/article/33/9/1639/2463654 by guest on 25 April 2024

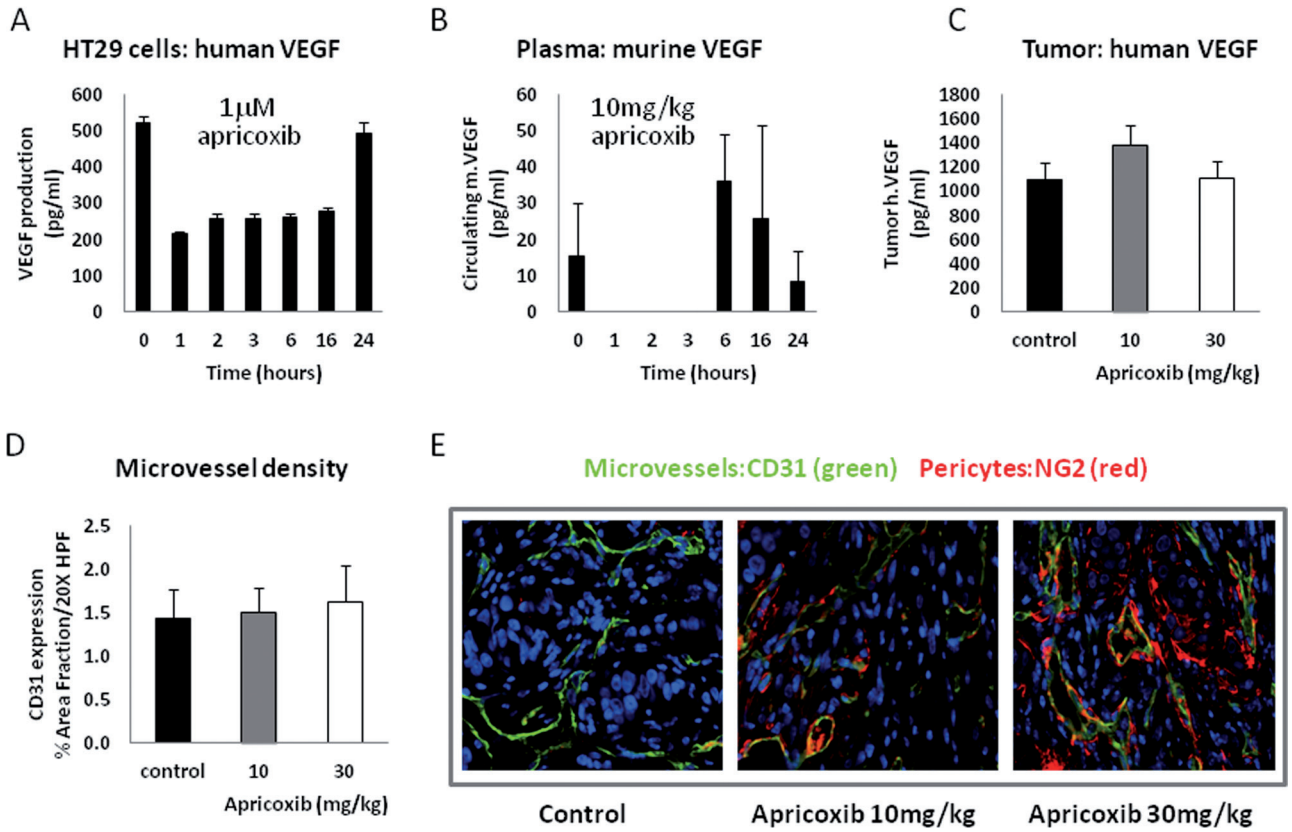

Fig. 4. Apricoxib modulates VEGF levels *in vitro* and *in vivo.* **(A)** The effect of 1 μM apricoxib on human VEGF production *in vitro* was assessed by ELISA. **(B)** HT29 tumor-bearing mice received a single oral dose of 10 mg/kg apricoxib and plasma was collected at various times thereafter and assayed for murine VEGF by ELISA (R&D Systems). **(C–E)** HT29 tumor-bearing mice were treated with vehicle or apricoxib (oral, daily 21×) and tumors were excised, lysed and assayed for human VEGF by ELISA **(C)** or were fixed, embedded and stained with antibodies to CD31 **(green)** and NG2 **(red),** quantification of microvessel density is displayed as mean ± SEM **(D)** and were analyzed as described in the legend to Fig. 1(B). Representative images of CD31 and NG2 in tumors from mice treated with control or apricoxib (10 and 30 mg/kg) are shown **(E)**, total magnification ×400.

levels are used as a surrogate for PGE_2 production (23,46–48), and we found that COX-2 levels were decreased *in vivo* after treatment with apricoxib. Given the submicromolar concentration of apricoxib present during dosing intervals, it is plausible that the therapeutic activity of apricoxib in this model was mediated by indirect effects on the host–tumor relationship, such as inhibition of angiogenesis (11). However, when we dissected the events occurring in treated tumors, it was evident that (i) tumor cell proliferation and survival were strongly inhibited, (ii) these effects could not be attributed to blockade of neovascularization, which did not occur in this model and (iii) the phenotype of the cells had changed during establishment of the xenografted tumors, including an EMT. These observations suggested that the adaptation of HT29 cells to *in vivo* tumor growth might lead to an increased dependency on COX-2 signaling for growth and survival, so we tested the apricoxib sensitivity of cells cultured under conditions that mimic the stresses of solid tumor growth. Under anchorage-independent growth conditions in soft agar clonogenic assays, HT29 cells displayed a markedly increased sensitivity to the drug with an IC_{50} of ~0.5 μM and complete killing was achieved at 5 μM. Similarly, culture conditions that stimulate EMT dramatically sensitized HT29 cells to the antiproliferative and proapoptotic effects of COX-2 inhibition. Interestingly, HT29 cells have relatively low COX-2 activity under resting conditions, but messenger RNA and protein expression are strongly induced by hypoxia, providing a plausible mechanism for heightened COX-2 dependency in the current studies (32). These observations were extended to NSCLC cells: although none were potently inhibited in monolayer culture (mean IC_{50} ~70 μM), 4/6 NSCLC lines were sensitive to apricoxib under anchorage-independent conditions. Notably, only those lines expressing ZEB-1 and displaying a mesenchymal phenotype were affected, suggesting that both EMT and stressful growth conditions contribute to COX-2-dependence in both cell types (25). In contrast, apricoxib levels required to cause the potential off-target effects seen in monolayer assays were not achieved *in vivo*. Celecoxib has been reported to also inhibit carbonic anhydrase and PDK1 (16). Apricoxib shares with celecoxib the sulfonamide moiety shown to mediate binding to carbonic anhydrase (18), but this activity is thought not to be responsible for tumor cell killing at mid-micromolar concentrations (33). Conversely, apricoxib was found not to inhibit any oncogenic kinases at 10 μM (31). These results indicate that apricoxib exerts antitumor activity via inhibition of COX-2-dependent PGE_2 production and possesses an unanticipated tumor cell-autonomous mode of action.

As previously reported for this (19) and other (4) COX-2 inhibitors, apricoxib did modulate VEGF expression *in vitro* and *in vivo*, with attendant changes to the tumor vasculature. Aberrant angiogenic signaling within tumors produces tortuous, permeable vessels resulting in increased interstitial fluid pressure and heterogeneous flow that drives tumor progression and reduces the delivery of chemotherapy. Although overall vessel density was unchanged, apricoxib treatment improved vessel maturity as indicated by increased pericyte coverage. Pericytes are critical in vessel stabilization, detachment of pericytes from endothelial cells occurs early in tumor angiogenesis allowing endothelial cell migration, increased vessel permeability and extravasation of metastatic cells into circulation (34). Several classes of antiangiogenic therapeutics, including previous COX-2 inhibitors (35), have been shown to induce vascular normalization, which results in decreased tumor hypoxia, vessel permeability and improved delivery of chemoradiation.

EMT is a developmental program that permits normally polarized, basement membrane-attached epithelial cells to undergo a series of biochemical alterations that allow them to assume a mesenchymal

Downloaded from https://academic.oup.com/carcin/article/33/9/1639/2463654 by guest on 25 April 2024

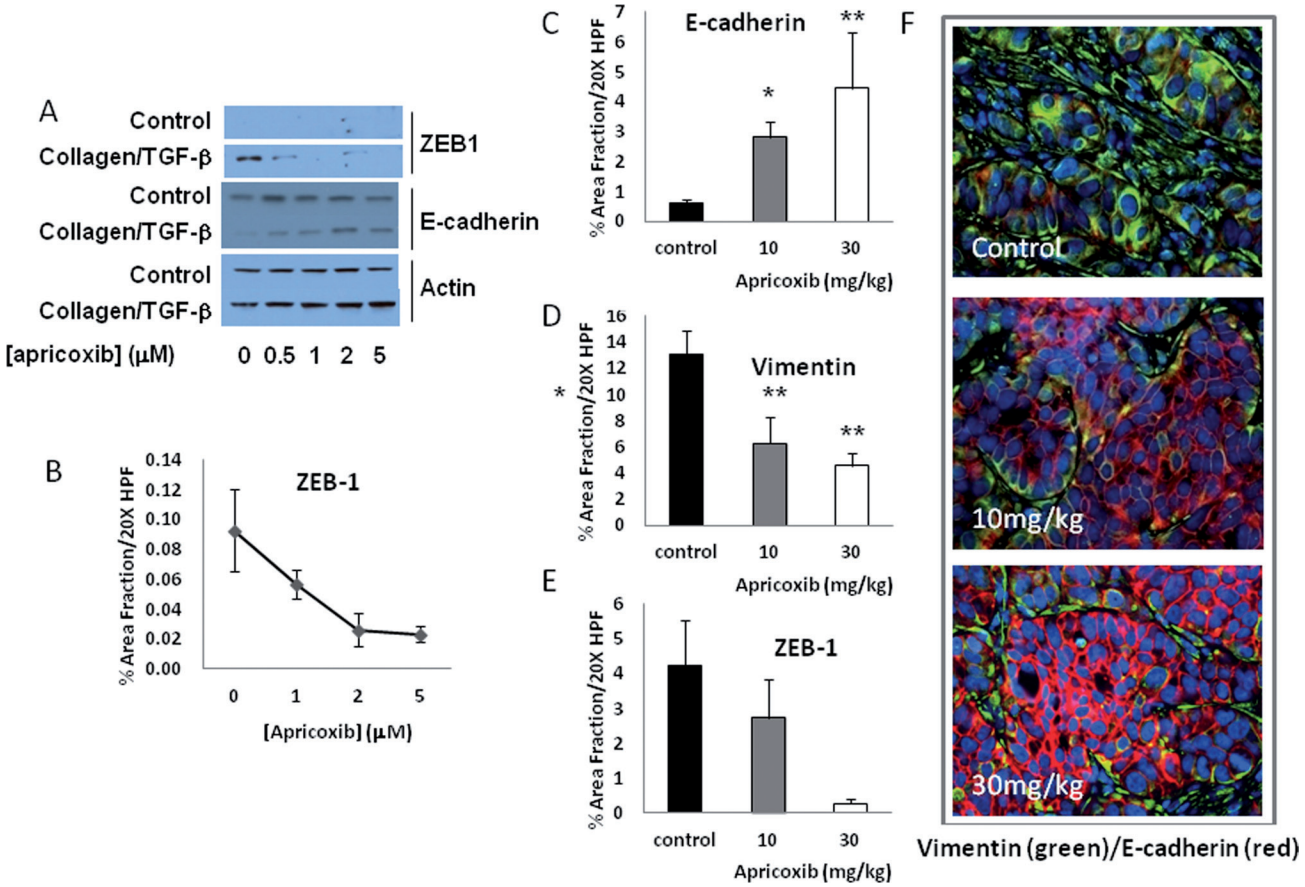

Fig. 5. Apricoxib reverses EMT. The effects of apricoxib on expression of epithelial (E-cadherin) and mesenchymal (ZEB1) markers *in vitro* was assessed by western blot **(A)** or immunocytochemistry **(B)** in cultures of HT29 cells grown under standard conditions or following growth on a collagen matrix in the presence of 20 ng/ml TGF-β. **(C–F)** HT29 tumor-bearing mice were treated with vehicle or apricoxib (oral, daily 21×) and tumors were stained with an antibodies against E-cadherin **(C,F)**, vimentin **(D,F)** or ZEB-1 **(E)**. Data are displayed as mean ± SEM and were analyzed as described in the legend to Fig. 1 (B); $*P \leq 0.0003$, $**P \leq 0.02$, $***P \leq 0.05$ versus control by one-way ANOVA. Representative double-stained images are also shown **(F)**.

phenotype characterized by loss of homotypic and matrix adhesion, increased invasiveness and resistance to apoptosis (36). In chronic inflammation and cancer, the EMT program is commonly subverted, driving tumor progression, metastatic spread and drug resistance (1,36). A recent study reported that most adenocarcinomas and squamous cell carcinomas of the lung are EMT^+ (42). Many of the properties of cancer cells that have undergone EMT are also associated with COX-2 hyperactivity (3,37). Furthermore, PGE_2 has been shown to induce EMT in CRC and NSCLC cells via upregulation of the transcription factors Snail and ZEB1 (21) and enhance TGF-β-induced EMT in mammary epithelial cells (38). In this study, we show that (i) HT29 cells undergo EMT when grown subcutaneously in nude mice, (ii) apricoxib robustly reverses this process *in vivo* (and *in vitro* at pharmacologically relevant concentrations) and (iii) reversal of EMT *in vitro* and *in vivo* is associated with inhibition of tumor cell proliferation and survival. Although EMT is most often linked to invasion and metastasis, our data suggest that EMT reversal by apricoxib also profoundly affects primary tumor growth. EMT has also been strongly linked to the acquisition by epithelial cancer cells of 'stem-like' properties, such as enhanced self-renewal capability and resistance to chemotherapy (39). Although the nature of cancer stem cells remains controversial, tumor-initiating cells in CRC have been shown to express the stem cell marker CD133 (30), and apricoxib significantly depleted CD133+ cells from HT29 tumors (data not shown), perhaps also explaining the reduced tumor cell proliferation and survival seen *in vivo*. An important role for PGE_2 in embryonic and hemopoietic stem cell homeostasis has recently been described (29,40,41). Our data suggest that inhibition of COX-2, probably via reversal of EMT, selectively depleted self-renewing stem cells from HT29 xenografts *in vivo*, a finding with important implications for the use of COX-2 inhibitors in cancer therapy.

In summary, we present evidence that the clinical stage COX-2 inhibitor apricoxib exerts direct and indirect anticancer effects in CRC and NSCLC models via inhibition of COX-2-dependent PGE_2 production. We propose that the ability of the drug to impact several 'hallmarks of cancer' may be secondary to reversal of EMT, an oncogenic process that appears to increase COX-2 dependence. EMT increases resistance to many therapeutic agents, including erlotinib (37,43), so it is notable that apricoxib has recently been found to be active in NSCLC in combination with erlotinib (44). Our data suggests that inhibition of the COX-2 pathway could add to the clinical benefit of both targeted anticancer agents and chemotherapy in several solid tumor types.

Supplementary material

Supplementary Tables 1 and 2, and Figure 1 can be found at http://carcin.oxfordjournals.org/

Funding

A sponsored research agreement from Tragara and the Effie Marie Cain Scholarship in Angiogenesis Research (to R.A.B) and an institutional training grant from the NCI (T32 CA136515 to A.K.).

Conflicts of interest statement: S.Z. and F.J.B. are employees of Tragara Pharmaceuticals.

Downloaded from https://academic.oup.com/carcin/article/33/9/1639/2463654 by guest on 25 April 2024

References

1. Hanahan,D. *et al*. (2011) Hallmarks of cancer: the next generation. *Cell*, **144**, 646–674.
2. Sobolewski, C. *et al*. (2010) The role of cyclooxygenase-2 in cell proliferation and cell death in human malignancies. *Int. J. Cell Biol.,* Article ID 215158.
3. Wang,D. *et al*. (2010) Eicosanoids and cancer. *Nat. Rev. Cancer*, **3**, 181–193.
4. De Groot,D.J. *et al*. (2007) Non-steroidal anti-inflammatory drugs to potentiate chemotherapy effects: from lab to clinic. *Crit. Rev. Oncol. Hematol*., **61**, 52–69.
5. Park,S.W. *et al*. (2011) The effects of the stromal cell-derived cyclooxygenase-2 metabolite prostaglandin E2 on the proliferation of colon cancer cells. *J. Pharm. Exper. Therap.,* **336**, 516–523.
6. Méric,J.B. *et al*. (2006) Cyclooxygenase-2 as a target for anticancer drug development. *Crit. Rev. Onc./Hem*., **59**, 51–64.
7. Krysan,K. *et al*. (2005) Prostaglandin E2 activates mitogen-activated protein kinase/Erk pathway signaling and cell proliferation in non-small cell lung cancer cells in an epidermal growth factor receptor-independent manner. *Cancer Res*., **65**, 6275–6281.
8. Wang,D. *et al*. (2005) Prostaglandin E2 enhances intestinal adenoma growth via activation of the Ras-mitogen-activated protein. *Cancer Res*., **65**, 1822–1829.
9. Castellone,M.D. *et al*. (2005) Prostaglandin E2 promotes colon cancer cell growth through a Gs-axin-beta-catenin signaling axis. *Science*, **310**, 1504–1510.
10. Chen,W. *et al.*. (2010) Acquired activation of the Akt/cyclooxygenase-2/Mcl-1 pathway renders lung cancer cells resistant to apoptosis. *Mol. Pharm.,* **77**, 416–423.
11. Williams,C.S.*et al*. (2000) Celecoxib prevents tumor growth *in vivo* without toxicity to normal gut: lack of correlation between *in vitro* and *in vivo* models. *Cancer Res.,* **60**, 6045–6051.
12. Trifan,O.C. *et al*. (2002) Cyclooxygenase-2 inhibition with celecoxib enhances antitumor efficacy and reduces diarrhea side effect of CPT-11. *Cancer Res*., **62**, 5778–5784.
13. Schiffmann,S.*et al*. (2008) The anti-proliferative potency of celecoxib in not a class effect of coxibs. *Biochem. Pharm*., **76**, 179–187.
14. Kazanov,D. *et al*. (2004) Celecoxib but not rofecoxib inhibits the growth of transformed cells *in vitro*. *Clin Cancer Res*., **10**, 267–271.
15. Paulson,S.K. *et al*. (2001) Pharmacokinetics of celecoxib after oral administration in dogs and humans: effect of food and site of absorption. *J. Pharm. Exp. Ther*., **297**, 638–645.
16. Arico,S. *et al*. (2002) Celecoxib induces apoptosis by inhibiting 3-phosphoinositide-dependent protein kinase-1 activity in the human colon cancer. *J. Biol. Chem*., **277**, 27613–27621.
17. http://clinicaltrials.gov/ct2/results?term=apricoxib
18. Ushiyama,S. *et al*. (2008) Preclinical pharmacology profile of CS-706, a novel cyclooxygenase-2 selective inhibitor, with potent antinociceptive and anti-inflammatory effects. *Eur. J. Pharm*., **578**, 76–86.
19. Senzaki,M. *et al*. (2008) CS-706, a novel cyclooxygenase-2 selective inhibitor, prolonged the survival of tumor-bearing mice when treated alone or in combination with anti-tumor chemotherapeutic agents. *Int. J. Cancer*, **122**, 1384–1390.
20. Reckamp,K. *et al*. (2011) Biomarker-based phase I dose-escalation, pharmacokinetic, and pharmacodynamic study of oral apricoxib in combination with erlotinib in advanced non small cell lung cancer. *Cancer*, **117**, 809–818.
21. Dohadwala,M. *et al*. (2006) Cyclooxygenase-2-dependent regulation of E-cadherin: prostaglandin E2 induces transcriptional repressors ZEB1 and snail in non-small cell lung cancer. *Cancer Res*., **66**, 5338–5345.
22. Doherty,G.A. *et al*. (2009) Proneoplastic effects of PGE2 mediated by EP4 receptor in colorectal cancer. *BMC Cancer*, **9**, 207–239.
23. Narayanan,B.A. *et al*. (2003) Suppression of N-methyl-N-nitrosourea/testosterone-induced rat prostate cancer growth by celecoxib: effects on cyclooxygenase-2, cell cycle regulation, and apoptosis mechanism(s). *Clin Cancer Res*., **9**, 3505–3513.
24. Wild,R.P. *et al*. (2006) Cetuximab preclinical antitumor activity (monotherapy and combination based) is not predicted by relative total or activated epidermal growth factor receptor tumor expression levels. *Mol. Cancer Ther*., **324**, 104–113.
25. Takeyama,Y. *et al*. (2010) Knockdown of ZEB1, a master epithelial-to-mesenchymal transition (EMT) gene, suppresses anchorage-independent cell growth of lung cancer cells. *Cancer Lett*., **296**, 216–224.
26. Gotoh,N. *et al*. (2007) An in vitro model of posterior capsular opacity: SPARC and TGF-beta2 minimize epithelial-to-mesenchymal transition in lens epithelium. *Invest Ophthalmol. Vis. Sci*., **48**, 4679–4687.
27. Reinmuth,N. *et al*. (2002) Blockade of insulin-like growth factor 1 receptor function inhibits growth and angiogenesis of colon cancer. *Clin. Cancer Res*., **8**, 3259–3269.
28. Jang,T.J. *et al*. (2009) Cycloxygenase-2 expression is related to the epithelial-to-mesenchymal transition in human colon cancers. *Yonsei Med. J*., **50**, 818–824.
29. Wellner,U. *et al*. (2009) The EMT-activator ZEB1 promotes tumorigenicity by repressing stemness-inhibiting microRNAs. *Nature Cell Biol*., **11**, 1487–1495.
30. Ricci-Vitiani,L. *et al*. (2007) Identification and expansion of human colon-cancer-initiating cells. *Nature*, **445**, 111–115.
31. Investigator's Brochure. *Investigational Product: Apricoxib Tablets*. Tragara Pharmaceuticals 2008.
32. Kaidi,A. *et al*. (2006) Direct transcriptional up-regulation of cyclooxygenase-2 by hypoxia-inducible factor (HIF)-1 promotes colorectal tumor cell survival and enhances HIF-1 transcriptional activity during hypoxia. *Cancer Res*., **66**, 6683–6691.
33. Grösch,S. *et al*. (2006) Cyclooxygenase-2 (COX-2) – independent anticarcinogenic effects of selective COX-2 inhibitors. *J. Natl. Cancer Inst*., **98**, 736–747.
34. Goel,S. *et al*. (2011) Normalization of the vasculature for treatment of cancer and other diseases. *Physiol. Rev*., **91**, 1071–1121.
35. Wagemakers,M. *et al*. (2009) COX-2 inhibition combined with radiation reduces orthotopic glioma outgrowth by targeting the tumor vasculature. *Translat. Oncol*., **2**, 1–7.
36. Kalluri,R. *et al*. (2009) The basics of epithelial-mesenchymal transition. *J. Clin. Invest*., **119**, 1420–1428.
37. Krysan,K. *et al*. (2008) Inflammation, epithelial to mesenchymal transition, and epidermal growth factor receptor tyrosine kinase inhibitor resistance. *J. Thorac. Oncol*., **3**, 107–110.
38. Neil,J.R. *et al*. (2008) Cox-2 inactivates Smad signaling and enhances EMT stimulated by TGF-ß through a PGE2-dependent mechanisms. *Carcinogenesis*, **29**, 2227–2235.
39. Singh,A. *et al*. (2010) EMT, cancer stem cells and drug resistance: an emerging axis of evil in the war on cancer. *Oncogene*, **29**, 4741–4751.
40. Goessling,W. *et al*. (2009) Genetic interaction of PGE2 and Wnt signaling regulates developmental specification of stem cells and regeneration. *Cell*, **136**, 1136–1147.
41. North,T.E. *et al*. (2007) Prostaglandin E2 regulates vertebrate haematopoietic stem cell homeostasis. *Nature*, **447**, 1007–1011.
42. Prudkin,L. *et al*. (2009) Epithelial-to-mesenchymal transition in the development and progression of adenocarcinoma and squamous cell carcinoma of the lung. *Mod. Pathol*., **22**, 668–678.
43. Thomson,S. *et al*. (2005) Epithelial to mesenchymal transition is a determinant of sensitivity of non-small-cell lung carcinoma cell lines and xenografts to epidermal growth factor receptor inhibition. *Cancer Res*., 9455–9462.
44. Gitlitz,B. *et al*. (2012) APRICOT-L: results of a biomarker based phase II randomized placebo-controlled study of apricoxib in combination with erlotinib in non-small cell lung cancer (NSCLC) patients. *J. Thoracic Oncol*., in press.
45. Arnold,S. *et al*. (2010) Lack of host SPARC enhances vascular function and tumor spread in an orthotopic murine model of pancreatic carcinoma. *Dis. Model Mech*., **3**, 57–72.
46. Faour,W. *et al*. (2001) Prostaglandin E2 regulates the level and stability of cyclooxygenase-2 mRNA through activation of p38 mitogen-activated protein kinase in interleukin-1 treated human synovial fibroblasts. *J. Biol. Chem*., **276**, 1720–1731.
47. Masferrer,J.L. *et al*. (1994) Selective inhibition of inducible cyclooxygenase 2 in vivo is anti-inflammatory and nonulcerogenic. *Proc. Natl. Acad. Sci*., **91**, 3228–3232.
48. Yoshinaka,R. *et al*. COX-2 inhibitor celecoxib suppresses tumor growth and lung metastasis of a murine mammary cancer. *Anticancer Res*., **26**, 4245–4254.

Received January 23, 2012; revised April 17, 2012; accepted May 26, 2012

Downloaded from https://academic.oup.com/carcin/article/33/9/1639/2463654 by guest on 25 April 2024